doi:10.1093/brain/awq028 Brain 2010: 133; 1054–1066 | 1054

BRAIN
A JOURNAL OF NEUROLOGY

T cells can mediate viral clearance from ependyma but not from brain parenchyma in a major histocompatibility class I- and perforin-independent manner

Daniel D. Pinschewer,[1,2] Mariann Schedensack,[3] Andreas Bergthaler,[1,2,4] Edit Horvath,[2] Wolfgang Brück,[3] Max Löhning[5] and Doron Merkler[3]

1 Department of Pathology and Immunology, W.H.O. Collaborating Centre for Neonatal Vaccinology, University of Geneva, Geneva, Switzerland
2 Institute of Experimental Immunology, Department of Pathology, University Hospital of Zurich, Zurich, Switzerland
3 Department of Neuropathology, Georg August University Goettingen, Goettingen, Germany
4 Institute for Systems Biology, Seattle/WA, USA
5 Experimental Immunology, Department of Rheumatology and Clinical Immunology, Charité—University Medicine Berlin and German Rheumatism Research Centre (DRFZ), Berlin, Germany

Correspondence to: Doron Merkler,
Department of Neuropathology,
Georg August University Goettingen,
Robert-Koch-Str. 40, 37099 Goettingen,
Germany
E-mail: merkler@med.uni-goettingen.de

Viral infection of the central nervous system can lead to disability and death. Yet the majority of viral infections with central nervous system involvement resolve with only mild clinical manifestations, if any. This is generally attributed to efficient elimination of the infection from the brain coverings, i.e. the meninges, ependyma and chorioplexus, which are the primary targets of haematogeneous viral spread. How the immune system is able to purge these structures from viral infection with only minimal detrimental effects is still poorly understood. In the present work we studied how an attenuated lymphocytic choriomeningitis virus can be cleared from the central nervous system in the absence of overt disease. We show that elimination of the virus from brain ependyma, but not from brain parenchyma, could be achieved by a T cell-dependent mechanism operating independently of major histocompatibility class I antigens and perforin. Considering that cytotoxic T lymphocyte-mediated cytotoxicity is a leading cause of viral immunopathology and tissue damage, our findings may explain why the most common viral intruders of the central nervous system rarely represent a serious threat to our health.

Keywords: cellular immune response; cytotoxic T-cell response; infection of the nervous system; choriomeningitis; virus; T cells

Abbreviations: LCMV = lymphocytic choriomeningitis virus; MHC = major histocompatibility complex; NP = nucleoprotein; RAG = recombination-activating gene; rLCMV/INDG = recombinant LCMV expressing the surface glycoprotein of vesicular stomatitis virus

Received September 17, 2009. Revised January 8, 2010. Accepted January 19, 2010
© The Author (2010). Published by Oxford University Press on behalf of the Guarantors of Brain. All rights reserved.
For Permissions, please email: journals.permissions@oxfordjournals.org

Introduction

Viruses are the most common infectious intruders to the CNS and remain a significant source of neurological morbidity and mortality worldwide. The United States Centres for Disease Control and Prevention estimate that ~20 000 cases of clinically manifested viral CNS infections occur in the United States each year. In addition, and vastly exceeding these numbers, many of the common viral infections 'silently' (i.e. in the absence of clinical symptoms or overt disease) involve the CNS, or exhibit mild manifestations that do not require diagnostic or therapeutic intervention. Hence, they are not included in the above statistics (Logan and MacMahon, 2008). Mumps in the pre-vaccine era is a classic example of a viral infection frequently accompanied by meningitis. CNS involvement occurred in an estimated 50% of all infected individuals but mostly went unrecognized and resolved without complications or sequelae (Johnstone *et al*., 1972; Hviid *et al*., 2008). Similar frequencies of CNS involvement were observed during acute but uncomplicated systemic infection with measles (Gibbs *et al*., 1959; Hanninen *et al*., 1980). Clinically, investigation of the topic has been hampered by the fact that it requires sampling of CSF, an intervention difficult to justify given the mostly benign and spontaneous outcome. Hence, similarly frequent mild CNS involvement as in measles and mumps is also suspected for other viruses such as influenza virus (Fujimoto *et al*., 1998) or coxsackie B virus (Rubin *et al*., 1958), which are nowadays more widespread. However, laboratory confirmation is not available.

Viral infections of the CNS are classified pathologically into those restricted to the parenchyma (encephalitis) and those that predominantly affect the coverings of the CNS (i.e. meninges, ependyma and chorioplexus), although some overlap of these categories is frequently observed. The majority of viral CNS infections result from haematogeneous dissemination and are initially confined to the CNS coverings (Fields *et al*., 2006). Often clinically manifested as 'aseptic meningitis', this syndrome summarizes a group of disorders with a typically mild and self-limiting course of disease (Adair *et al*., 1953; Irani, 2008). It is generally assumed that immunocompetent individuals eliminate these infections from the CNS coverings before a substantial parenchymal infection can be established, and thus before substantial damage occurs. Furthermore, properties intrinsic to the virus (cellular tropism, cytolytic potential) and host parameters such as age (e.g. neonatal versus adult life, thereby affecting the level of immunological competence) influence whether the virus remains restricted to the brain coverings or whether it also affects the CNS parenchyma. Numerous DNA and RNA viruses including enteroviruses, morbilliviruses, herpes viruses, lentiviruses, flaviviruses and arenaviruses are able to spread into the brain coverings in humans (Lee and Davies, 2007). How they gain access to the CNS has been studied extensively, and much effort has been given to elucidating virus-host interactions and immune defence in the brain parenchyma (Griffin, 2003; Hausmann *et al*., 2005; McGavern, 2005; Bergmann *et al*., 2006; Ercolini and Miller, 2006; Tishon *et al*., 2006). However, less is known about how infected hosts silently cleanse the CNS coverings from viral infection, and thus how they prevent not only serious complications from meningitis, but also viral spread into the parenchyma.

Lymphocytic choriomeningitis virus (LCMV) represents the prototypic member of the arenavirus family and is widely used to study the dichotomous role of the antiviral immune response in host protection and pathogenesis (Zinkernagel and Doherty, 1974; Ahmed and Gray, 1996; Oldstone, 2007). LCMV is a natural mouse pathogen but it is also suspected to be an underestimated cause of aseptic meningitis in humans (Meyer *et al*., 1960; Jahrling and Peters, 1992). As in humans, LCMV has the capacity to infect the brain coverings of mice, and from there it gradually spreads into the parenchyma (Thomsen, 2009). Intracerebral inoculation of adult mice with LCMV has been studied for decades to define the mechanisms underlying viral pathogenesis and immunopathology in the CNS. After intracerebral administration most of the inoculum is drained into the systemic circulation (Mims, 1960), initiating a vigorous immune response. At the same time, the virus replicates in the leptomeninges, choroid plexus and ependymal cells (Lillie, 1945; Wilsnack and Rowe, 1964). LCMV is non-cytolytic in mice, and hence the ensuing CNS disease is solely caused by the immune response attacking the virus infection in the CNS. Accordingly, T cell-depleted mice are resistant to LCMV-induced fatal choriomeningitis (Cole *et al*., 1972). Histological examination shows massive leucocyte infiltrates accumulating in the meningeal and ventricular region of the brain 6–8 days after infection, concomitant with the onset of rapidly progressing convulsions and death. In addition to these events in the brain coverings, T cell infiltration has also been observed within the brain parenchyma, and clinical disease has mostly been attributed to the latter part of the inflammatory response (Christensen *et al*., 2004). $CD8^+$ T cells have long been identified as key players indispensable for disease (Cole *et al*., 1972; Andersen *et al*., 1991). Yet recently the recruitment of myelomonocytic cells was also found to be an important step in pathogenesis (Kim *et al*., 2009), at least for the early manifestation of the disease.

In contrast to the vast majority of humans with viral infection of the CNS surface, intracerebral infection of mice with wild-type LCMV strains is almost invariably lethal, even at the minimal infectious dose (Bonilla *et al*., 2002). Thus, acute LCMV meningitis in mice is only of limited use for investigating how a primary immune response can purge viruses from the brain coverings without causing overt disease.

Therefore, using arenavirus reverse genetics, we recently generated an attenuated LCM virus exhibiting a fundamentally different virus–host balance: recombinant LCMV expressing the surface glycoprotein of vesicular stomatitis virus (rLCMV/INDG) instead of its own glycoprotein (Fig. 1A). Unlike wild-type LCMV such as the Armstrong strain, rLCMV/INDG fails to cause disease in intracerebral-infected adult mice (Pinschewer *et al*., 2003; Bergthaler *et al*., 2006; Merkler *et al*., 2006). Nevertheless, it establishes persistent infection in the CNS of immunodeficient hosts (Merkler *et al*., 2006) owing to its non-cytolytic behaviour. As an additional important difference to wild-type LCMV, rLCMV/INDG replicates only in the CNS. Even in recombination-activating gene (RAG)-deficient mice lacking T and B cells, interferon type I prevents viral replication in other tissues (Merkler *et al*., 2006). In several other model systems, viral elimination from the CNS can

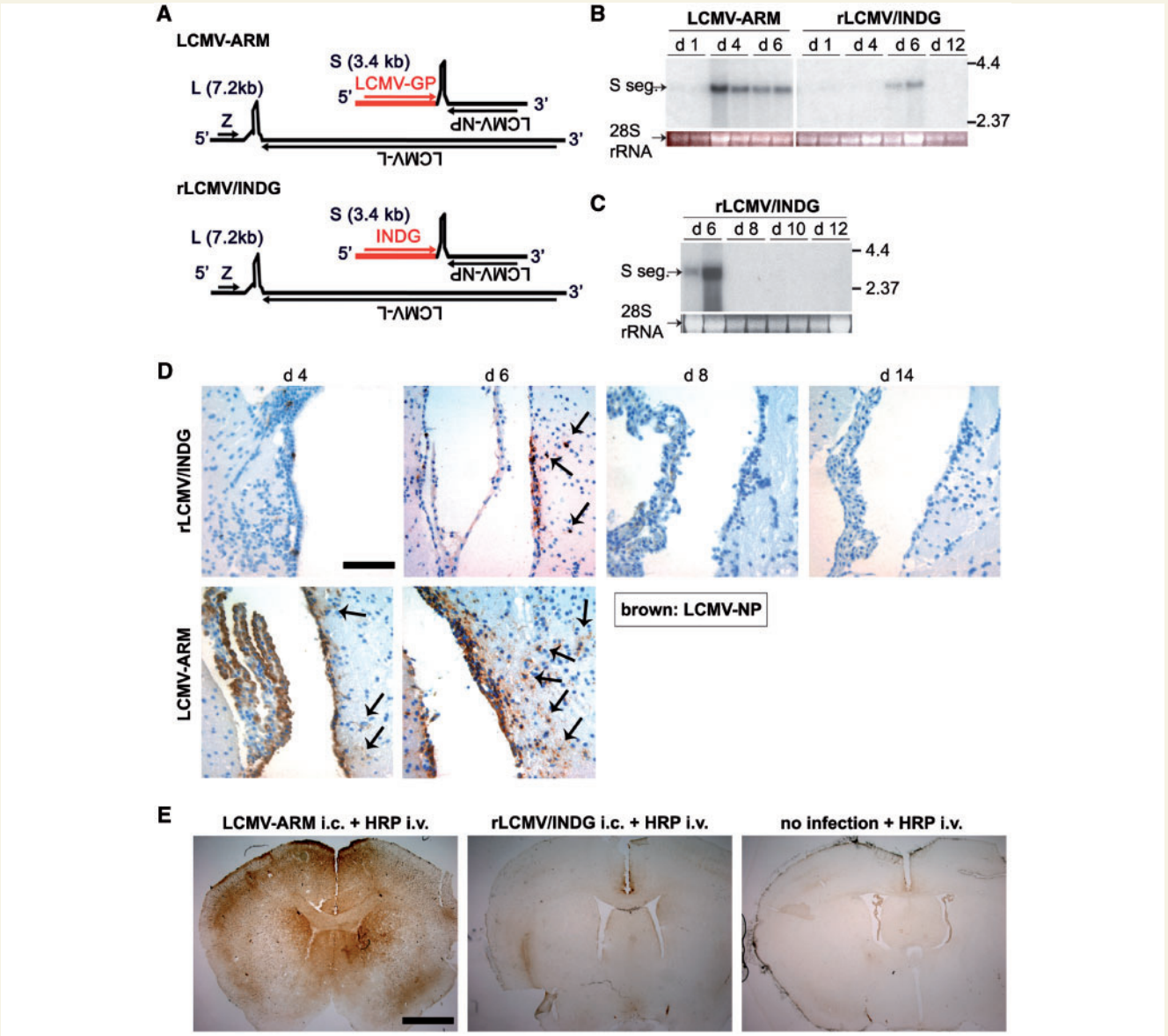

Figure 1 Genome organization, viral spread and blood brain barrier integrity following intracerebral infection with either LCMV Armstrong or rLCMV/INDG. (**A**) Schema of the LCMV-Armstrong (LMCV-ARM) and rLCMV/INDG genomes. Both viruses consist of two single-stranded negative-strand RNA segments, encoding two viral genes in ambisense orientation each. The long (L) segment encodes for the RNA-dependent RNA polymerase L and for the matrix protein Z, while the short (S) segment carries the *GP* and *NP* genes. rLCMV/INDG was created by substituting the LCMV-GP gene for vesicular stomatitis virus-INDG (Pinschewer *et al*., 2003). (**B–E**) C57BL/6 mice were infected intracerebrally with rLCMV/INDG or LCMV-ARM as indicated or were left uninfected. (**B** and **C**) Viral S-segment (S seg.) RNA in brain was detected at the indicated day (d) after intracerebral infection by northern blot (ethidium bromide staining of 28S rRNA indicates loading control; lanes represent individual animals). (**D**) Immunohistochemical detection of LCMV-NP confirms reduced spread of rLCMV/INDG as compared to LCMV-Armstrong. Note that LCMV- Armstrong (Days 4 and 6) and also rLCMV/INDG (Day 6) spreads into some subependymal cells (arrows). (**E**) At Day 6 after infection, animals were given horseradish peroxide (HRP) intravenously. One hour later, they were sacrificed for detection of horseradish peroxidase leakage into the brain parenchyma, indicative of blood brain barrier breakdown. Representative pictures of horseradish peroxidase reactions are shown ($n = 3$–4 animals per group). Scale bar for **D**: 100 μm; for **E**: 500 μm.

be affected by ongoing viral replication at additional sites, particularly when the virus overwhelms the host to cause immune exhaustion (Wherry and Ahmed, 2004). Thus the rLCMV/INDG model is well suited to study viral CNS clearance in mouse models with defects in adaptive immunity.

In the present work we used this experimental model to dissect the individual contribution of key components and pathways of the adaptive immune response in purging a non-cytolytic virus infection from the CNS in the absence of severe disease. Our results indicate that viral elimination from ependymal cells can be achieved in a T cell-dependent manner that occurs independently of major histocompatibility complex (MHC) class I and perforin, whereas the cytolytic mechanisms of cytotoxic T cells become essential once the virus has gained access to the parenchyma, notably to glial cells.

Materials and methods

Mice

C57BL/6 wild-type mice, recombination activation gene 2 deficient mice ($RAG^{-/-}$(Chen *et al*., 1993*a*)), B cell deficient mice ($JHT^{-/-}$ (Chen *et al*., 1993*b*)), T cell deficient mice ($TCR\beta\delta^{-/-}$ (Mombaerts *et al*., 1994)), major histocompatibility complex (MHC) class I-deficient ($\beta2m^{-/-}$ (Koller *et al*., 1990) and $K^bD^{b-/-}$ (Perarnau *et al*., 1999)), major histocompatibility complex class II deficient mice $MHCII^{-/-}$ (Kontgen *et al*., 1993), perforin deficient mice PKO (Kagi *et al*., 1994), TNF receptor double deficient mice ($TNFR1/2^{-/-}$ (Peschon *et al*., 1998)), FAS deficient mice ($FAS^{-/-}$ (Adachi *et al*., 1995)), CD8 deficient mice ($CD8^{-/-}$ (Fung-Leung *et al*., 1991)) and interferon gamma deficient (GKO (Dalton *et al*., 1993)) mice (on C57BL/6 background) as well as 129Sv/Ev wild-type mice and interferon gamma receptor deficient mice ($IFNGR^{-/-}$ (Huang *et al*., 1993)) on a 129Sv/Ev background were bred at the Institute of Laboratory Animal Science, University of Zurich and housed under specific pathogen-free conditions during all experiments. Animal experiments were carried out at the University of Zurich with authorization by the cantonal veterinary office and in accordance with the Swiss law for animal protection, and at the University of Göttingen with the authorization by the district government in Braunschweig, in accordance with the German law for animal protection.

Viruses, virus titrations, inoculations and determination of neutralizing antibodies

Virus stocks were prepared, infectivity was quantified and vesicular stomatitis virus neutralizing antibodies were determined as described previously (Pinschewer *et al*., 2004). For intracerebral inoculations, 3×10^3 plaque forming units of the Armstrong strain of LCMV or rLCMV/INDG were administered in a volume of 30 µl through the vertex of the skull using a 27 gauge needle. For intravenous infection, 2×10^4 plaque forming units of the Armstrong strain of LCMV in a volume of 200 µl were administered into the tail vein. Vesicular stomatitis virus-hyperimmune serum (Pinschewer *et al*., 2004) was administered i.p.

Detection of viral RNA

Viral S segment (~3.4 kb) was detected by northern hybridization as described previously (Pinschewer *et al*., 2003). A quantitive TaqMan reverse transcribed (RT)-PCR protocol targeting the *LCMV-nucleoprotein* (*NP*) gene (to be described elsewhere) was used to quantify rLCMV/INDG S segment copies in the brain of infected mice. Arbitrary viral RNA units were determined in a multiplex assay with a commercial kit for detection of the housekeeping gene *GAPDH*, serving as internal reference (Applied Biosystems).

Cytotoxicity assays and enumeration of epitope-specific $CD8^+$ T cells

Specific cytotoxic T cell activity of splenocytes was assayed in a ^{51}Cr release assay and epitope-specific $CD8^+$ T cells were enumerated using MHC class I tetramers as described (Bergthaler *et al*., 2006).

Histopathology

CNS tissue was prepared in hepes-glutamic acid buffer-mediated organic solvent protection effect (HOPE) fixative (DCS Innovative) (Olert *et al*., 2001) and embedded in paraffin as described previously (Bergthaler *et al*., 2007). Mice were not perfused prior to tissue collection and fixation since rLCMV/INDG does not replicate outside the CNS, and blood contains neither free infectivity nor circulating infected cells (Merkler *et al*., 2006). Upon inactivation of endogenous peroxidases (phosphate buffered saline/0.3% hydrogen peroxide, 30 min) and blocking (phosphate buffered saline/10% foetal calf serum), sections were stained with primary antibodies: mouse anti-neuronal nuclei NeuN (Chemicon International), mouse anti-glial fibrillary acidic protein (astrocytes; Dako), mouse anti-NogoA [oligodendrocytes, mAb11c7 (Oertle *et al*., 2003), kindly provided by M. E. Schwab, Brain Research Institute, Zurich], rat anti-mouse CD8 (BD PharMingen), rabbit anti-ionized calcium binding adaptor-1 (microglia/macrophages; Wako Pure Chemical Industries Ltd.), rabbit anti-Factor VIII (von Willebrand Factor; endothelia; Abcam) and rat anti-LCMV NP (VL-4, Battegay *et al*., 1991). Bound primary antibodies were visualized either by an avidin-biotin technique with 3,3′-diaminobenzidine or alkaline phosphatase/anti-alkaline phosphatase as chromogens (haemalaun counterstaining of nuclei) for light microscopy or with the appropriate species-specific Cy3- or Cy2-conjugated secondary antibodies (all from Jackson ImmunoResearch Laboratories Inc.) with 4′,6-diamidino-2-phenylindole (Sigma-Aldrich) nuclei counterstaining for fluorescence microscopy. To assess cellular distribution of LCMV at least 130 LCMV-NP^+ cells per staining and group (average 416 ± 123 cells) were evaluated at ×400 magnification. Number of LCMV-NP^+ cells allocated to a given cellular subtypes were expressed as percent of total allocated LCMV NP^+ cells.

Assessment of blood brain barrier breakdown

Damage to the blood brain barrier was visualized by intravenous injection of 400 µl of 2% horseradish peroxidase (Sigma) dissolved in phosphate-buffered saline (Claudio *et al*., 1990; Hawkins *et al*., 1990). Horseradish peroxidase leakage into the brain parenchyma was made evident in horseradish peroxidase reactions on 6 µm-thick snap-frozen sections of brain tissue.

Statistical analysis

ANOVA with Bonferroni post test was used for the comparison of individual values from multiple groups. Viral RNA units were log-transformed for statistical analysis. Differences in individual values between two groups were analysed by *t*-tests (unpaired, two-tailed) and virus clearance was compared in log rank tests. These analyses were performed using GraphPad Prism software version 4.0b. Two-way ANOVA with Bonferroni's post test for a combined analysis of values from two groups in two independent experiments was performed using SPSS version 13.0. *P*-values <0.05 were considered statistically significant (*) and *P*-values <0.01 were considered highly significant (**), whereas *P*-values >0.05 were considered statistically not significant.

Results

Reduced spread of rLCMV/INDG in CNS coverings correlates with a largely intact blood brain barrier

We first infected mice intracerebrally with rLCMV/INDG or with its wild-type counterpart LCMV Armstrong, and compared the viral burden in CNS and its topographical distribution over time. Northern blot analysis of LCMV Armstrong-infected brain tissue detected similar amounts of viral RNA on Day 4 as on Day 6 when the animals displayed signs of terminal disease (Fig. 1B). In addition, LCMV Armstrong RNA was also detectable in spleen on Days 1 and 4 after infection (Supplementary Fig. S1). By the same methods, rLCMV/INDG RNA became detectable no earlier than at Day 6, and was eliminated by Day 8 (Fig. 1B and C). In agreement with our previous findings (Merkler *et al*., 2006), rLCMV/INDG RNA could not be detected in spleen or liver at any time point (Supplementary Fig. S1). Northern hybridization had suggested lower levels of rLCMV/INDG than of Armstrong in the CNS (Fig. 1B), which was confirmed by histological analysis (Fig. 1D). Both viruses were mostly restricted to the brain coverings (i.e. leptomeninges, ependyma and chorioplexus). However, rLCMV/INDG infected far fewer cells than Armstrong, both on Day 4 and 6 after infection. rLCMV/INDG was found in small foci and in isolated infected cells of leptomeninges and ependyma on Day 4, in somewhat larger patches of infected cells of the same structures on Day 6 after infection, and was cleared thereafter (Days 8 and 14, Fig. 1D). In contrast, as early as on Day 4 Armstrong-infected cells formed a continuous layer comprising meninges, ependymal cells and choroid plexus. Furthermore, a small but consistent fraction of parenchymal cells in close proximity to the ventricular ependyma (referred to as 'subependymal cells') were also infected, as previously reported (Christensen *et al*., 2004) (arrows in Fig. 1D). We further analysed the integrity of the blood brain barrier at Day 6 after infection with either LCMV Armstrong or rLCMV/INDG. This time point was chosen for analysis since rLCMV/INDG RNA levels and T cell infiltrates were highest (Fig. 1B and text below) and also because of terminal disease in LCMV Armstrong-infected animals (Fig. 1E). Extensive disruption of the blood brain barrier was found in LCMV Armstrong infection, which was evident in widespread leakage of intravenously administered horseradish peroxidase into the brain parenchyma, confirming earlier observations in LCMV-infected mice (Marker *et al*., 1984; Andersen *et al*., 1991). In contrast, the blood brain barrier was only very modestly affected in rLCMV/INDG-infected animals. rLCMV/INDG is known to persist in the brain of immunodeficient hosts, such as neonates, without causing disease (Pinschewer *et al*., 2003; Bergthaler *et al*., 2006; Merkler *et al*., 2006). Hence the present data indicate that adult infection of mice with rLCMV/INDG provides a useful model to study basic mechanisms of silent immune-mediated viral clearance from the brain coverings.

The benign course of intracerebral rLCMV/INDG infection is not due to an altered antiviral cytotoxic T cell response

We had previously demonstrated that the failure of rLCMV/INDG to elicit fatal choriomeningitis was not due to its lack of LCMV glycoprotein (Fig. 1A) as an antigenic target of the cytotoxic T cell response to LCMV Armstrong (Bergthaler *et al*., 2006). We had also shown that intracerebral rLCMV/INDG infection induces cytotoxic T cell responses of high frequency and long-lived protective capacity (Bergthaler *et al*., 2006). Yet LCMV Armstrong-induced cytotoxic T cells reached even higher frequencies and exhibited far higher cytotoxic activity in primary *ex vivo* cytotoxic T cell assays (Pinschewer *et al*., 2004). This difference in cytotoxic T cell response rather than the viral ability to spread in the CNS could thus have accounted for the differential clinical outcome after rLCMV/INDG and LCMV Armstrong infection. To address this possibility, we infected mice simultaneously with rLCMV/INDG and/or LCMV Armstrong using the intracerebral and intravenous routes in various combinations (Fig. 2A). Besides recording the clinical outcome (Fig. 2A), we used MHC class I tetramers to

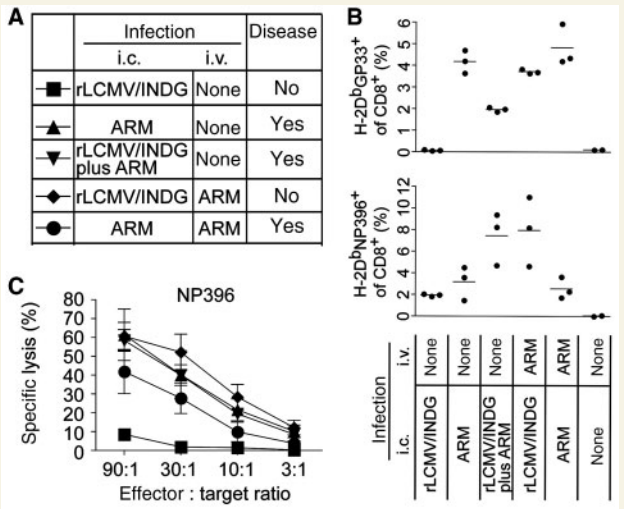

Figure 2 Absence of disease after rLCMV/INDG intracerebral infection is not due to altered antiviral cytotoxic T cell response. (**A**) C57BL/6 mice were infected by the intravenous and intracerebral route with LCMV-Armstrong (LCMV-ARM) and/or rLCMV/INDG in various combinations as indicated in the chart, summarizing also the clinical outcome of infection. Animals exhibiting clinical signs of terminal choriomeningitis were euthanized in accordance with the Swiss law for animal protection. (**B**) NP396-specific (expressed by both viruses) and GP33-specific (expressed by LCMV-ARM) $CD8^+$ T cells in blood were enumerated on Day 6 by MHC class I tetramer staining. (**C**) Primary *ex vivo* cytotoxic T cell activity of splenocytes against NP396 was tested 6 days after infection. Symbols represent the mean ± SEM of three mice per group. Symbol keys are provided in the table of panel A.
i.c. = intracerebral; i.v. = intravenous.

monitor the magnitude of the antiviral cytotoxic T cell response (Fig. 2B), and its cytolytic activity was determined in primary *ex vivo* cytotoxic T cell assays (Fig. 2C). Co-infection with rLCMV/INDG intracerebral and Armstrong intracerebral resulted in lethal choriomeningitis analogous to Armstrong intracerebral single infection. This excluded dominant negative immunomodulatory effects of rLCMV/INDG on CNS immunopathogenesis. Furthermore we found that intracerebral administration of Armstrong caused the same T cell response and disease regardless of whether or not Armstrong was additionally administered intravenously. Thus, we tested whether Armstrong intravenous infection could drive a cytotoxic T cell response of optimal magnitude and cytolytic capacity that would trigger CNS disease in animals simultaneously infected with intracerebral rLCMV/INDG. Although the magnitude and functionality of the peripheral antiviral cytotoxic T cell response was equivalent or even slightly higher than in Armstrong single-infected mice, these animals failed to display evidence of increased morbidity, both by clinical assessment and also by testing blood brain barrier permeability analogous to the experiments displayed in Fig. 1E (data not shown). Hence, these results confirm that the ability of LCMV Armstrong but not rLCMV/INDG to cause CNS disease is unrelated to differences in the cytotoxic T cell response elicited, but rather reflect differential viral load and/or distribution in CNS tissues.

T cells—but not antibodies—are necessary to clear recombinant LCMV/INDG from the CNS

Next we analysed the contribution of the adaptive cellular and humoral immune response to silent rLCMV/INDG clearance from the CNS. B cell-deficient JHT$^{-/-}$ mice exhibited unimpaired virus clearance whereas the brains of T cell-deficient TCR$\beta\delta^{-/-}$ mice and RAG$^{-/-}$ animals (lacking T as well as B cells) harboured considerable levels of persisting virus as assessed on Day 14 of infection and thereafter (Fig. 3A and data not shown). The antiviral CD8$^+$ T cell response to the immunodominant epitope NP396 was measured in peripheral blood on Day 8 using MHC class I tetramers (Fig. 3B). These responses were similarly vigorous in mice with a targeted deletion of the JH locus (JHT mice) lacking B cells, and C57BL/6 control mice, but were absent in CD8$^+$ T cell-deficient TCR$\beta\delta^{-/-}$ and RAG$^{-/-}$ mice, as expected, and therefore correlated with viral clearance. Notably, rLCMV/INDG intracerebral infection also elicited a vigorous and early virus-neutralizing antibody response (Fig. 3C and D). Its absence in JHT mice did not change the clinically silent course of rLCMV/INDG infection (not shown), indicating that silent clearance of rLCMV/INDG but not LCMV Armstrong was unrelated to differences in the virus-neutralizing antibody responses elicited by the two viruses. It also suggested that antibodies were not essential for rLCMV/INDG clearance from the CNS, but a contributory role in this process was not excluded. TCR$\beta\delta^{-/-}$ not only failed to mount cytotoxic T cell responses but in addition they displayed considerably reduced total virus-neutralizing antibody titres (IgM plus IgG, $P<0.01$) and a virtual absence of the β-mercaptoethanol-resistant virus-neutralizing antibody fraction (IgG, $P<0.01$). This was presumably due to the lack of T cell help for antibody production and immunoglobulin class switch, and could also have contributed to defective viral clearance in these animals. To address this possibility, we reconstituted TCR$\beta\delta^{-/-}$ animals with specific antibodies by intraperitoneal administration of hyperimmune serum (Fig. 3E–G). While neutralizing IgG in serum was restored to virtually normal levels, viral persistence remained unaffected. In summary, these findings indicate that T cells play an essential role in the silent clearance of rLCMV/INDG from the CNS, a process that largely occurs independently of systemic antiviral antibodies.

Clearance of LCMV/INDG from the CNS is dependent on MHC class I and perforin

Considering the key role of T cells in the clearance process, we dissected the contribution of MHC class I- (MHCI-) and class II- (MHCII-) restricted responses in rLCMV/INDG clearance from the brain. Three of four MHC class I-deficient (MHCI$^{-/-}$) mice exhibited rLCMV/INDG RNA on Day 14 after infection whereas in mice lacking MHC class II (MHCII$^{-/-}$) virus was undetectable (Fig. 4A). The differential ability to eliminate rLCMV/INDG from the CNS correlated with the normal generation of virus-specific CD8$^+$ T cells in MHCII$^{-/-}$ mice, whereas MHCI$^{-/-}$ mice are devoid of a CD8$^+$ T cell compartment (Fig. 4B). Unlike in the experiment depicted in Fig. 4A, a repeat experiment in MHCI$^{-/-}$ mice resulted in invariable viral persistence. Altogether, rLCMV/INDG persisted in six out of seven MHCI$^{-/-}$ mice tested, which was significantly different from the uniform clearance in C57BL/6 wild-type controls ($P<0.01$). To corroborate these findings in an independent knockout mouse model, we assessed rLCMV/INDG clearance from the CNS of CD8$^{-/-}$ mice, which also lack MHCI-restricted T cells. Virus persisted in the brains of all four CD8$^{-/-}$ infected mice, further supporting a key role of MHCI-restricted T cell responses in rLCMV/INDG clearance from the CNS (Fig. 4C and D, $P<0.0001$ for a combined analysis of virus clearance in C57BL/6 versus CD8$^+$ T cell-deficient MHCI$^{-/-}$ and CD8$^{-/-}$ mice). As a next step we analysed the individual contribution of Fas, perforin, interferon-γ and tumour necrosis factor-α for eliminating rLCMV/INDG (Figs 4E–H and Supplementary Fig. S2). Unimpaired virus control in mice lacking either tumour necrosis factor receptors 1 and 2 (TNFR1/2$^{-/-}$), FAS (FAS$^{-/-}$), interferon-γ (GKO) or interferon-γ receptor contrasted with clearly detectable viral persistence in the brain of six out of eight perforin-deficient mice tested in two independent experiments (Fig. 4E and H; data not shown; $P<0.01$ for virus clearance in perforin-deficient mice versus C57BL/6 control mice). Impaired clearance of virus from the CNS of perforin-deficient mice was accompanied by normal frequencies of viral epitope-specific CD8$^+$ T cells in peripheral blood ($P=0.69$ for NP396-specific CD8+ T cell frequencies in perforin-deficient mice versus C57BL/6 mice; combined analysis of Figs 4F and I), as expected (Badovinac *et al*., 2002). This indicated that it was indeed the absence of perforin-dependent cytolytic pathways rather than a general impairment of CD8$^+$ T cell

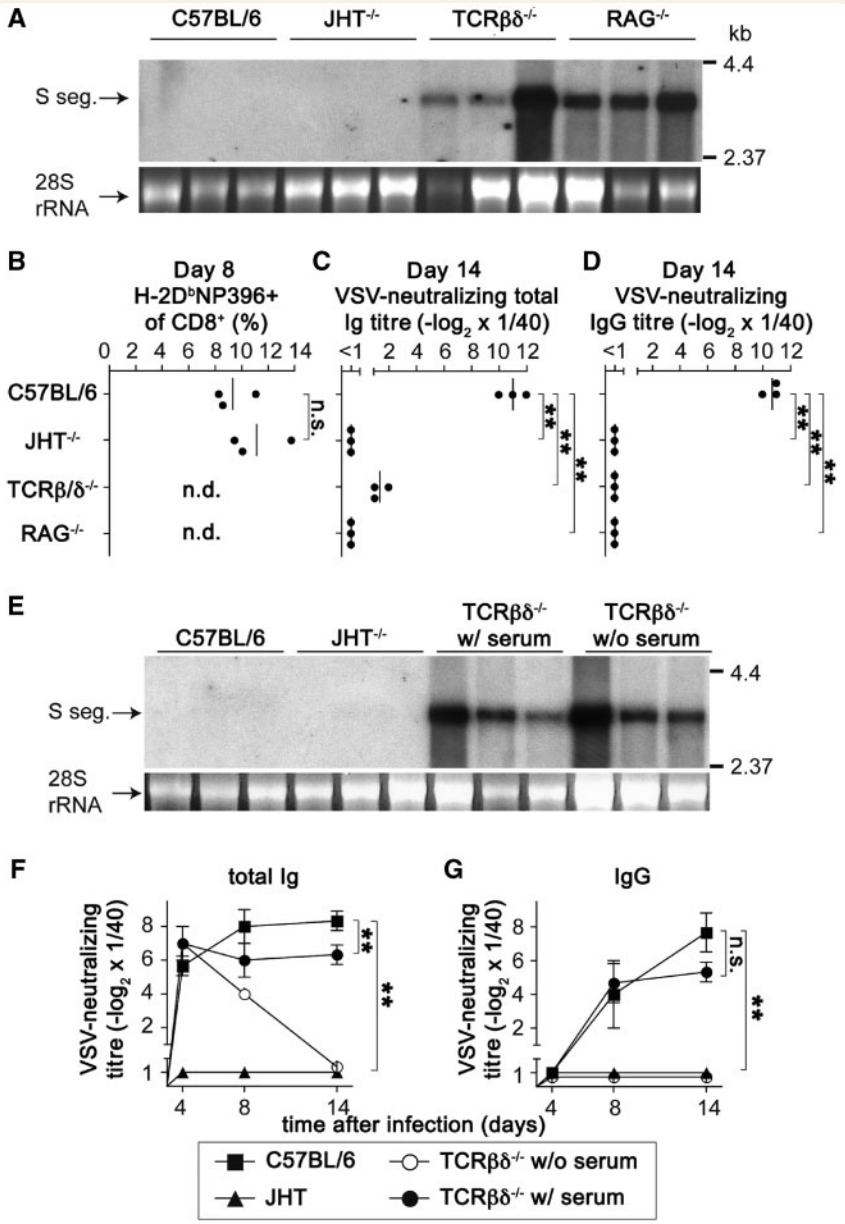

Figure 3 T cells—but not antibodies—are necessary for clearance of rLCMV/INDG from the CNS. Mice of the indicated genotypes were infected with rLCMV/INDG intracerebrally. (**A**) Detection of viral S-segment (S seg.) RNA in the brain by northern blot on Day 14 (ethidium bromide staining of 28S rRNA indicates loading control). (**B**) Frequencies of NP396-specific $CD8^+$ T cells in blood were determined on Day 8 using MHC class I tetramers. $TCR\beta\delta^{-/-}$ and $RAG^{-/-}$ mice lack $CD8^+$ T cells. (**C** and **D**) Virus-neutralizing total Ig (**C**) and IgG (**D**) were determined at the indicated time points. (**E–G**) C57BL/6, JHT and $TCR\beta\delta^{-/-}$ mice were infected as above. An additional group of $TCR\beta\delta^{-/-}$ mice was treated with 500 μl of vesicular stomatitis virus-immune serum on Day 7. (**E**) Viral RNA in the brain was detected on Day 14 by northern hybridization. (**F** and **G**) Virus neutralizing total Ig and IgG titres in serum were determined over time. Lanes in **A** and **E** and symbols in **B–D** represent individual mice. Symbols in **F–G** represent the mean ± SEM of three mice per group. Representative results from two similar experiments are shown. n.d. = not detectable; n.s. = not significant ($P > 0.05$); ** = highly significant ($P < 0.01$).

responses that caused viral persistence in the CNS of perforin-deficient mice.

To gain further insights on how rLCMV/INDG persisted in the CNS of perforin-deficient, $TCR\beta\delta^{-/-}$ and $RAG^{-/-}$ mice but not in C57BL/6 controls, we performed histological time course analyses of viral antigen and of infiltrating $CD8^+$ T cells. Four days after infection the virus was restricted to ependymal cells from where it spread into a few subependymal cells by Day 6 (Fig. 5A). These early events were identical in T cell-competent perforin-deficient and wild-type animals as well as in T cell-deficient $TCR\beta\delta^{-/-}$ and $RAG^{-/-}$ mice. However, C57BL/6 wild-type animals eliminated the virus by Day 8, whereas slowly but steadily increasing numbers of infected cells were found within the CNS parenchyma of perforin-deficient, $TCR\beta\delta^{-/-}$ and $RAG^{-/-}$ mice on Days 8, 10

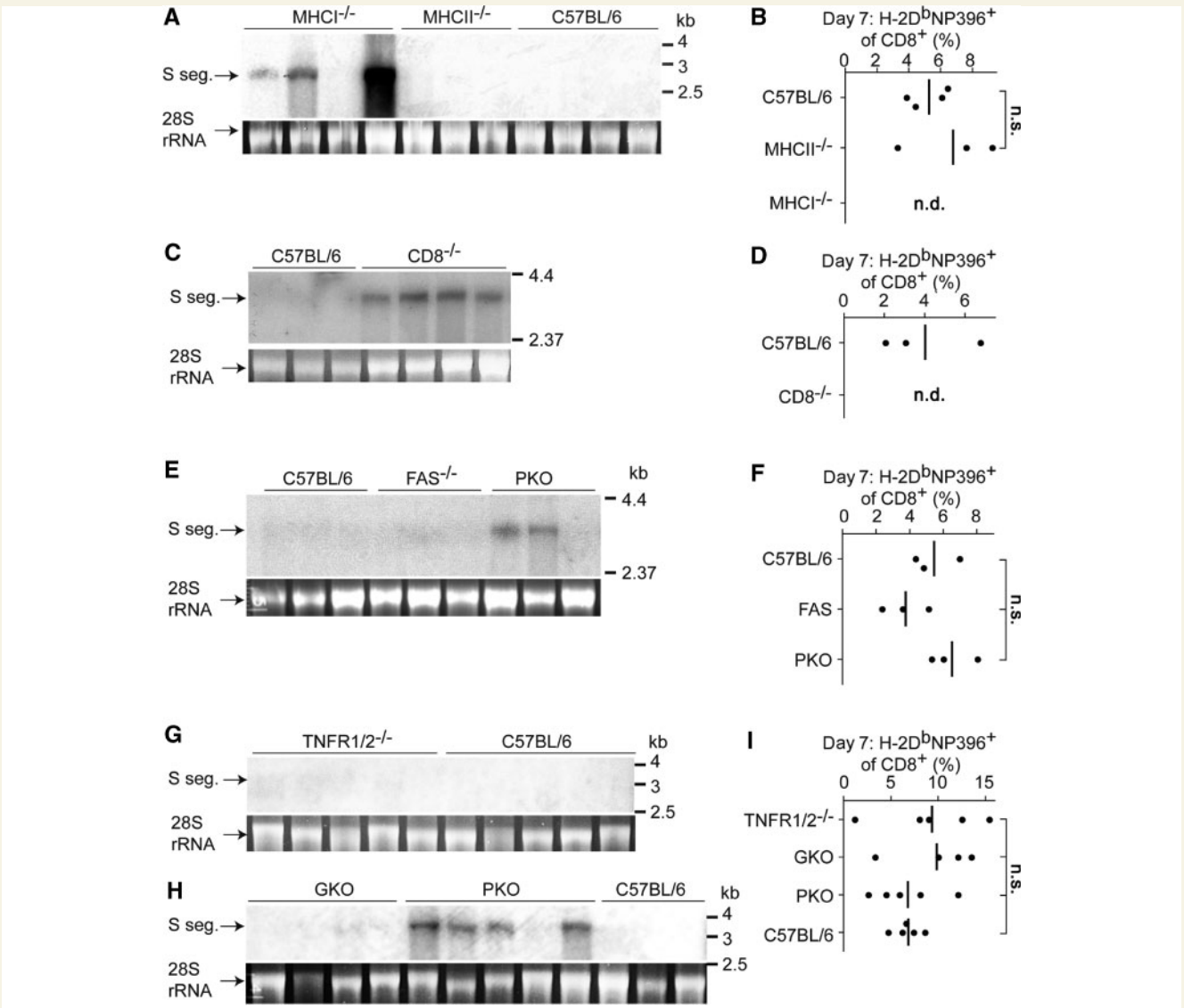

Figure 4 Clearance of LCMV/INDG from the CNS is dependent on MHC class I and perforin. Mice of the indicated genotypes were infected with rLCMV/INDG intracerebrally. (**A**, **C**, **E**, **G** and **H**) Viral S-segment (S seg.) RNA was detected by northern blot on Day 14 after intracerebral infection. Ethidium bromide staining is shown as loading control. (**B**, **D**, **F** and **I**) NP396-specific $CD8^+$ T cell frequencies in blood were enumerated at Day 7 after infection. $MHCI^{-/-}$ mice and $CD8^{-/-}$ mice lack $CD8^+$ T cells. Symbols and lanes represent individual mice. In figure **F** and **I**, multiple comparisons were not performed since the *F*-test of ANOVA failed to detect significant differences ($P > 0.05$). n.d. = not detectable; n.s. = not significant ($P > 0.05$).

and 12. Comparable virus dissemination in these three knockout strains of mice supported the notion that perforin- and MHCI-dependent T cell control was primarily responsible for preventing persistence of rLCMV/INDG in the brain parenchyma. The failure of perforin-deficient mice to clear rLCMV/INDG was not due to a potential delay or impairment of $CD8^+$ T cell trafficking to infected brain regions (Fig. 5B). In C57BL/6 mice, as in perforin-deficient mice, infiltrating $CD8^+$ T cells were first detected on Day 6 in similar numbers. Unlike in wild-type controls, where cytotoxic T cell infiltration in the meninges and periventricular areas peaked at this time point and declined thereafter, cytotoxic T cell infiltrates in perforin-deficient mice increased even further at Days 8, 10 and 12, presumably as a result of persisting viral antigen. In summary, these data show that MHCI-restricted perforin-dependent mechanisms play a key role in the silent clearance of rLCMV/INDG from the CNS.

Virus clearance from parenchyma—but not from ependyma—depends on MHC class I and perforin

The above analyses demonstrated similar dissemination of rLCMV/INDG in the parenchyma of perforin-deficient, $TCR\beta\delta^{-/-}$ and $RAG^{-/-}$ mice. However, differential infection rates were noted in the ependyma of the different mouse strains (Fig. 5, insets in Day 12 images). Thus we studied the cell types in which rLCMV/INDG persisted when infected mice lacked either T or B cells

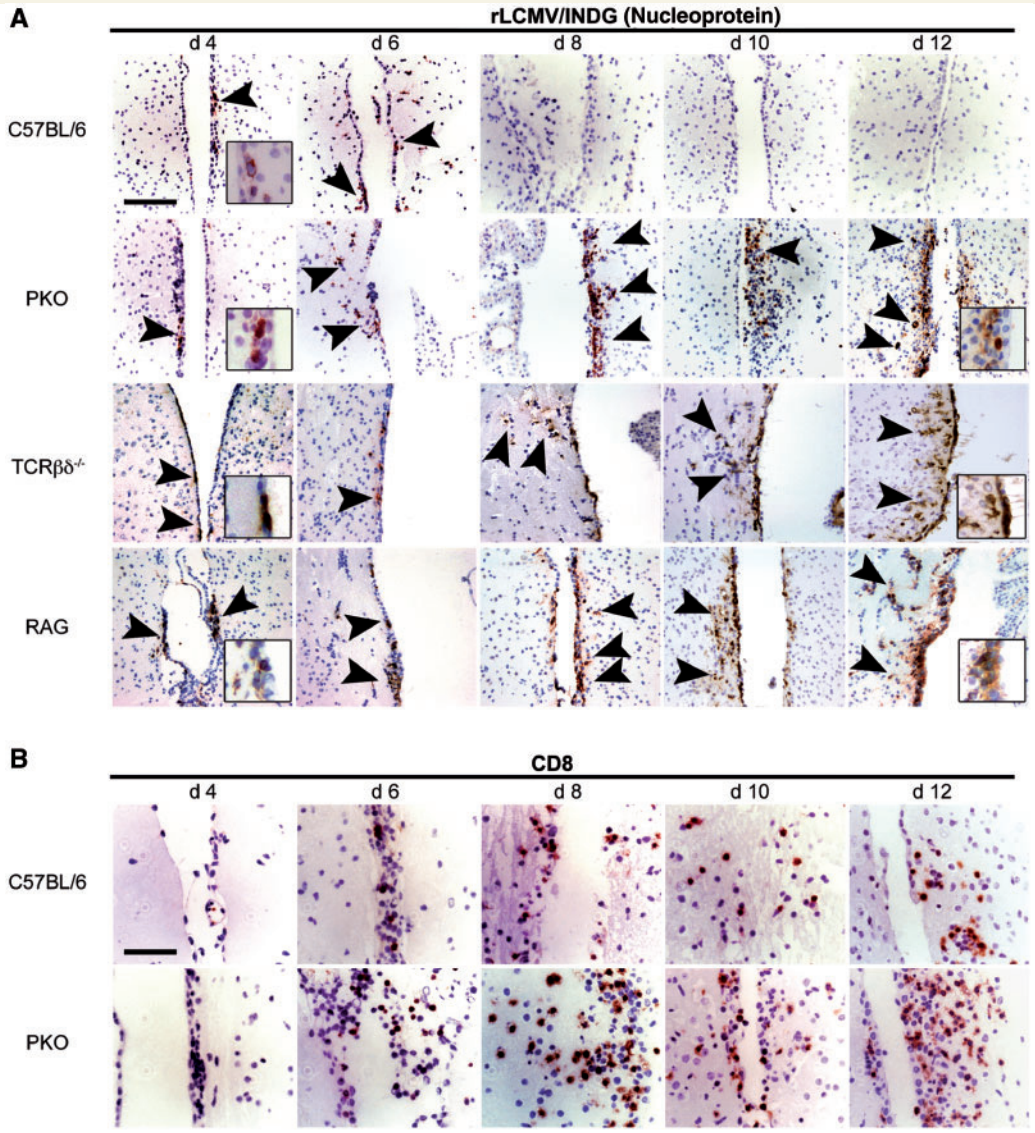

Figure 5 rLCMV/INDG dissemination in the brain of perforin-deficient, TCRβδ$^{-/-}$ and RAG$^{-/-}$ mice, and dense CD8^{+} T cell infiltrates in perforin-deficient mice. Perforin-deficient (PKO), TCRβδ$^{-/-}$, RAG$^{-/-}$ and C57BL/6 wild-type control mice were infected with rLCMV/INDG intracerebrally and were sacrificed at the indicated time points. Brain tissues were processed for immunohistochemical analysis of LCMV NP (**A**) and CD8^{+} T cells (**B**). The latter analysis was only performed for perforin-deficient and C57BL/6 mice since TCRβδ$^{-/-}$ and RAG$^{-/-}$ mice lack T cells. Representative images of 2–4 animals per group and timepoint are shown. Arrowheads in (**A**) indicate infected (LCMV NP-positive) subependymal cells. Insets in the Day 12 timepoints of (**A**) show persisting infection of ependymal cells in TCRβδ$^{-/-}$ and RAG$^{-/-}$ but not in perforin-deficient mice, whereas subependymal cells are infected in all three knockout strains. Scale bars **A**: 100 μm; **B**: 50 μm. d = days post intracerebral infection.

(RAG$^{-/-}$), the entire T cell compartment (TCRβδ$^{-/-}$), MHCI-restricted T cells (MHCI$^{-/-}$) or perforin as a key component of cytolytic CD8^{+} T cell activity. Immunohistochemical co-stains were performed 2 weeks after rLCMV/INDG infection using a LCMV NP-specific antibody in combination with cell type-specific markers (Fig. 6). Striking differences were noted in the ependyma on Day 14, and were further supported by the kinetic analysis of virus distribution depicted in Fig. 5. Unlike in the early phase of infection when the virus was mostly confined to the brain coverings (compare Figs 1D and 5), MHCI$^{-/-}$ and perforin-deficient animals displayed very few infected ependymal cells (MHCI$^{-/-}$ 5%, perforin-deficient 2%). In contrast, ependymal cells were the most frequently infected cell type (47%) in TCRβδ$^{-/-}$ mice and RAG-/- mice (48%). Within the parenchyma, a similar global picture was found in all four knockout mouse strains, with the majority of infected cells identified as astrocytes that were predominantly located in periventricular areas (67% of infected cells positive for glial fibrillary acidic protein in MHCI$^{-/-}$ mice; 60% in perforin-deficient, 31% in TCRβδ$^{-/-}$, 29% in RAG$^{-/-}$ mice). To a lesser degree, viral infection co-localized with the oligodendrocyte marker NogoA (MHCI$^{-/-}$ 14%, perforin-deficient 24%, TCRβδ$^{-/-}$ 8%, 14% in RAG$^{-/-}$ mice), with the neuronal marker

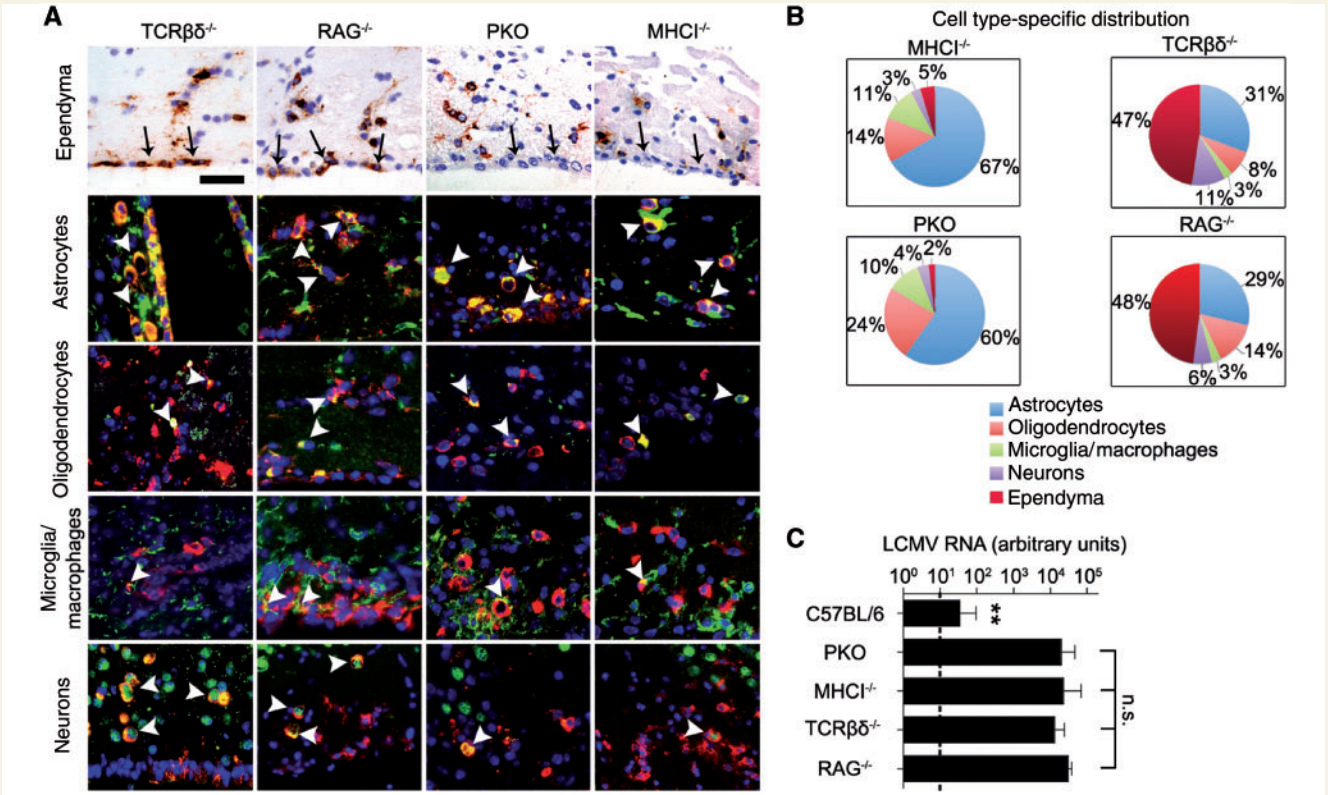

Figure 6 The cell type-specific distribution of rLCMV/INDG in the CNS is different in TCR$\beta\delta^{-/-}$ and RAG$^{-/-}$ mice as compared to perforin-deficient and MHCI$^{-/-}$ mice. Mice of the indicated genotypes were infected with rLCMV/INDG intracerebrally. Fourteen days later they were sacrificed and brain tissues were processed for histological analysis of LCMV NP. (**A**) Ependyma was differentiated based on morphological criteria (arrows in top panel) combined with immunohistochemical detection of LCMV NP (brown). Infection of parenychmal cell types (bottom panels) was detected by combining LCMV NP staining (red) with cell type-specific markers (green) in immunofluorescent co-staining as indicated. Arrowheads point out colocalization of cell type-specific markers with LCMV NP in immunofluorescence images. Representative images from three to four animals per group are shown. Scale bar: 50 μm. (**B**) Histological images were quantified to define the proportion of each cell type within the total population of infected cells. (**C**) Viral RNA loads in the brain of the indicated mouse strains were measured by quantitative RT-PCR and are displayed in arbitrary units (see 'Materials and methods' section). Bars represent the mean + SD of four to seven animals per group. Viral RNA loads in infected C57BL/6 mice were significantly different from perforin-deficient (PKO), MHCI$^{-/-}$, TCR$\beta\delta^{-/-}$ and RAG$^{-/-}$ mice ($P < 0.01$), whereas the latter four were not significantly different from each other ($P > 0.05$ for all comparisons). The technical background was determined in brain tissue of uninfected mice (mean of six animals indicated as dashed line), and was not significantly different from infected C57BL/6 wild-type mice ($P > 0.05$, not shown).

NeuN (MHCI$^{-/-}$ 3%, perforin-deficient 4%, TCR$\beta\delta^{-/-}$ 11%, 6% in RAG$^{-/-}$ mice) and with the microglia/macrophage marker ionized calcium binding adaptor-1 (MHCI$^{-/-}$ 11%, perforin-deficient 10%, TCR$\beta\delta^{-/-}$ 3%, 3% in RAG$^{-/-}$ mice). Infection of endothelial cells was not detected, even when assessed in RAG$^{-/-}$ mice (Supplementary Fig. S3), and endothelia were therefore not included in the above analyses. Taken together, these findings suggest that, unlike in the parenchyma where the cell type-specific distribution of virus is similar in all four genotypes of knockout mice tested, silent clearance from ependyma could occur in a MHCI- and perforin-independent yet T cell-dependent fashion. Total viral RNA loads in the brain of perforin-deficient, MHCI$^{-/-}$, TCR$\beta\delta^{-/-}$ and RAG$^{-/-}$ mice are similar as determined by quantitative RT-PCR (Fig. 6C), providing evidence that within the brain parenchyma, adaptive immune pathways other than MHCI- and perforin-dependent T cell clearance do not substantially influence rLCMV/INDG persistence. At the same time, these RT-PCR data suggest that viral RNA in the ependyma does not represent a major fraction of the total viral RNA accumulating in the CNS of TCR$\beta\delta^{-/-}$ and RAG$^{-/-}$ mice. This may suggest that ependymal cells are less permissive to viral RNA amplification than the parenchyma.

Discussion

In contrast to viral encephalitis (i.e. infection of the brain parenchyma), viral infections generally follow a benign course if predominantly confined to the brain coverings. The underlying reasons are still poorly understood. In the current study we used a panel of gene-targeted mice to study redundant and non-redundant arms of adaptive immunity in viral clearance from CNS coverings versus

parenchyma. The differences discovered here offer a possible explanation for the fundamentally different clinical manifestations of viral infection in these two CNS compartments.

Based on the present results and on earlier data, we suggest the following scenario for viral clearance in our model of 'aseptic meningitis'. Blood-borne virus initially spreads to the CNS coverings. Both LCMV Armstrong and rLCMV/INDG (albeit the latter to a lesser extent) will slowly but steadily invade the brain parenchyma, spreading from cell to cell. With the onset of the adaptive immune response, ependymal viral replication is cleared in a T cell-dependent manner but independently of MHCI and perforin, a non-cytolytic process causing only minimal clinical manifestations, if any. Astrocytes contribute to the formation of the blood brain barrier and are close to the CNS coverings, rendering them a first viral target in the parenchyma. This most likely explains the high rate of astrocyte infection in MHCI$^{-/-}$, PKO, TCR$\beta\delta^{-/-}$ and RAG$^{-/-}$ mice on Day 14 after infection (compare Fig. 6), an assumption that is supported by the finding that neuronal infection becomes more prominent with time (data not shown). A reductionist model suggests that the ensuing cytotoxic T cell response eliminates the infected astrocytes by MHCI-dependent, perforin-mediated cytotoxicity. Unlike clearance from the CNS coverings, this cytolytic process inflicts damage to the blood brain barrier (compare Fig. 1E) and, together with other factors such as the local inflammatory tissue response, will lead to breakdown of the blood brain barrier. It seems likely that, depending on the number of infected astrocytes in the blood brain barrier (i.e. virus load; high in LCMV Armstrong, low in rLCMV/INDG infection), the resulting damage to the blood brain barrier will vary, and thus also the extent of serum protein leakage into the parenchyma. Once a certain level is reached, increased intracranial pressure will lead to the classical clinical signs of meningitis including nausea, seizures and ultimately death (Doherty and Zinkernagel, 1974; Camenga *et al*., 1977; Andersen *et al*., 1991). In agreement with this scenario, Christensen and colleagues (2004) found that delayed recruitment and accumulation of cytotoxic T cells in the brain parenchyma caused a delay in the onset of disease in LCMV-infected CXCL10- or CXCR3-deficient mice, despite normal inflammatory cell recruitment to the brain coverings (Christensen *et al*., 2004).

The precise molecular mechanisms as to how T cells effect non-cytolytic clearance of the brain coverings remains to be addressed in future work. Its occurrence independent of MHCI suggests that MHCII-restricted T cell responses or non-classical T cells and their respective effector molecules may be involved.

Myelomonocytic cells have recently been identified as previously neglected players in LCMV-host interactions within the CNS, and aside from T cells, monocyte/macrophages were also found to accumulate in the CNS coverings during rLCMV/INDG clearance (data not shown). Their presence could be a simple consequence of inflammation but they may also contribute to clearance in a direct or indirect manner. The study of their contribution to viral clearance is complicated by considerable redundancy with other pathways, stepping in when myelomonocytic inflammatory cells are experimentally depleted (Kim *et al*., 2009). For similar reasons, it may be difficult to delineate the precise role of T cell effector pathways other than perforin that may contribute to clearance of rLCMV/INDG from the CNS parenchyma (Griffin, 2003). However, the contribution of these pathways, unlike that of perforin, may simply have remained undetected owing to a higher degree of redundancy.

The model of adult intracerebral infection with rLCMV/INDG offers several features that render it particularly amenable to the investigation of viral clearance in aseptic meningitis. The virus' non-cytolytic behaviour avoids complications related to viral spread in immunocompromised animals, and as reported here, its attenuation avoids the fatal immunopathological complications of wild-type LCMV infection (Cole and Nathanson, 1974). On the flip-side of the coin, cytopathic effects of viral infection may also contribute to the clinical picture of 'aseptic meningitis' and are not part of the model. Nonetheless, rLCMV/INDG infection is ideally suited for the investigation of silent clearance, the most frequent yet often neglected outcome of viral CNS infection.

The present data delineate a clear dichotomy in the mechanisms underlying virus clearance from CNS coverings and parenchyma. MHCI- and perforin-dependence of the latter, but not the former, provides one likely explanation for the most frequently self-limiting course of viral CNS infection.

Acknowledgements

We would like to thank C. Crozier and C. Bunker for critically reading the manuscript.

Funding

D.D.P. holds a stipendiary professorship of the Swiss National Science Foundation (No. PP00A-114913) and was supported by grant No. 3100A0-104067/1 of the Swiss National Science Foundation. A.B. is an EMBO long-term fellow and supported by the SSMBS foundation of the Swiss National Science Foundation. M.L. is a Lichtenberg fellow funded by the Volkswagen Foundation. D.M. was supported by the German Research Foundation, SFB-TR43 (Project B3), and by the Gemeinnützige Hertie Stiftung.

Supplementary material

Supplementary material is available at *Brain* online.

References

Adachi M, Suematsu S, Kondo T, Ogasawara J, Tanaka T, Yoshida N, et al. Targeted mutation in the Fas gene causes hyperplasia in peripheral lymphoid organs and liver. Nat Genet 1995; 11: 294–300.

Adair CV, Gauld RL, Smadel JE. Aseptic meningitis, a disease of diverse etiology: clinical and etiologic studies on 854 cases. Ann Intern Med 1953; 39: 675–704.

Ahmed R, Gray D. Immunological memory and protective immunity: understanding their relation. Science 1996; 272: 54–60.

Andersen IH, Marker O, Thomsen AR. Breakdown of blood-brain barrier function in the murine lymphocytic choriomeningitis virus infection

mediated by virus-specific CD8+ T cells. J Neuroimmunol 1991; 31: 155–63.

Badovinac VP, Porter BB, Harty JT. Programmed contraction of CD8(+) T cells after infection. Nat Immunol 2002; 3: 619–26.

Battegay M, Cooper S, Althage A, Banziger J, Hengartner H, Zinkernagel RM. Quantification of lymphocytic choriomeningitis virus with an immunological focus assay in 24- or 96-well plates. J Virol Methods 1991; 33: 191–8.

Bergmann CC, Lane TE, Stohlman SA. Coronavirus infection of the central nervous system: host-virus stand-off. Nat Rev Microbiol 2006; 4: 121–32.

Bergthaler A, Gerber NU, Merkler D, Horvath E, de la Torre JC, Pinschewer DD. Envelope exchange for the generation of live-attenuated arenavirus vaccines. PLoS Pathog 2006; 2: e51.

Bergthaler A, Merkler D, Horvath E, Bestmann L, Pinschewer DD. Contributions of the lymphocytic choriomeningitis virus glycoprotein and polymerase to strain-specific differences in murine liver pathogenicity. J Gen Virol 2007; 88: 592–603.

Bonilla WV, Pinschewer DD, Klenerman P, Rousson V, Gaboli M, Pandolfi PP, et al. Effects of promyelocytic leukemia protein on virus-host balance. J Virol 2002; 76: 3810–8.

Camenga DL, Walker DH, Murphy FA. Anticonvulsant prolongation of survival in adult murine lymphocytic choriomeningitis. I. Drug treatment and virologic studies. J Neuropathol Exp Neurol 1977; 36: 9–20.

Chen J, Lansford R, Stewart V, Young F, Alt FW. RAG-2-deficient blastocyst complementation: an assay of gene function in lymphocyte development. Proc Natl Acad Sci USA 1993a; 90: 4528–32.

Chen J, Trounstine M, Alt FW, Young F, Kurahara C, Loring JF, et al. Immunoglobulin gene rearrangement in B cell deficient mice generated by targeted deletion of the JH locus. Int Immunol 1993b; 5: 647–56.

Christensen JE, Nansen A, Moos T, Lu B, Gerard C, Christensen JP, et al. Efficient T-cell surveillance of the CNS requires expression of the CXC chemokine receptor 3. J Neurosci 2004; 24: 4849–58.

Claudio L, Kress Y, Factor J, Brosnan CF. Mechanisms of edema formation in experimental autoimmune encephalomyelitis. The contribution of inflammatory cells. Am J Pathol 1990; 137: 1033–45.

Cole GA, Nathanson N. Lymphocytic choriomeningitis. Pathogenesis. Prog Med Virol 1974; 18: 94–110.

Cole GA, Nathanson N, Prendergast RA. Requirement for theta-bearing cells in lymphocytic choriomeningitis virus-induced central nervous system disease. Nature 1972; 238: 335–7.

Dalton DK, Pitts-Meek S, Keshav S, Figari IS, Bradley A, Stewart TA. Multiple defects of immune cell function in mice with disrupted interferon-gamma genes. Science 1993; 259: 1739–42.

Doherty PC, Zinkernagel RM. T-cell-mediated immunopathology in viral infections. Transplant Rev 1974; 19: 89–120.

Ercolini AM, Miller SD. Mechanisms of immunopathology in murine models of central nervous system demyelinating disease. J Immunol 2006; 176: 3293–8.

Fields B, Knipe DM, Howley PM. Fields virology. Philadelphia, Pennsylvania, USA: Lippincott Wiliams & Wilkins; 2006.

Fujimoto S, Kobayashi M, Uemura O, Iwasa M, Ando T, Katoh T, et al. PCR on cerebrospinal fluid to show influenza-associated acute encephalopathy or encephalitis. Lancet 1998; 352: 873–5.

Fung-Leung WP, Schilham MW, Rahemtulla A, Kundig TM, Vollenweider M, Potter J, et al. CD8 is needed for development of cytotoxic T cells but not helper T cells. Cell 1991; 65: 443–9.

Gibbs FA, Gibbs EL, Carpenter PR, Spies HW. Electroencephalographic abnormality in "uncomplicated" childhood diseases. J Am Med Assoc 1959; 171: 1050–5.

Griffin DE. Immune responses to RNA-virus infections of the CNS. Nat Rev Immunol 2003; 3: 493–502.

Hanninen P, Arstila P, Lang H, Salmi A, Panelius M. Involvement of the central nervous system in acute, uncomplicated measles virus infection. J Clin Microbiol 1980; 11: 610–3.

Hausmann J, Pagenstecher A, Baur K, Richter K, Rziha HJ, Staeheli P. CD8 T cells require gamma interferon to clear borna disease virus from the brain and prevent immune system-mediated neuronal damage. J Virol 2005; 79: 13509–18.

Hawkins CP, Munro PM, MacKenzie F, Kesselring J, Tofts PS, du Boulay EP, et al. Duration and selectivity of blood-brain barrier breakdown in chronic relapsing experimental allergic encephalomyelitis studied by gadolinium-DTPA and protein markers. Brain 1990; 113 (Pt 2): 365–78.

Huang S, Hendriks W, Althage A, Hemmi S, Bluethmann H, Kamijo R, et al. Immune response in mice that lack the interferon-gamma receptor. Science 1993; 259: 1742–5.

Hviid A, Rubin S, Muhlemann K. Mumps. Lancet 2008; 371: 932–44.

Irani DN. Aseptic meningitis and viral myelitis. Neurol Clin 2008; 26: 635–55, vii–viii.

Jahrling PB, Peters CJ. Lymphocytic choriomeningitis virus. A neglected pathogen of man. Arch Pathol Lab Med 1992; 116: 486–8.

Johnstone JA, Ross CA, Dunn M. Meningitis and encephalitis associated with mumps infection. A 10-year survey. Arch Dis Child 1972; 47: 647–51.

Kagi D, Ledermann B, Burki K, Seiler P, Odermatt B, Olsen KJ, et al. Cytotoxicity mediated by T cells and natural killer cells is greatly impaired in perforin-deficient mice. Nature 1994; 369: 31–7.

Kim JV, Kang SS, Dustin ML, McGavern DB. Myelomonocytic cell recruitment causes fatal CNS vascular injury during acute viral meningitis. Nature 2009; 457: 191–5.

Koller BH, Marrack P, Kappler JW, Smithies O. Normal development of mice deficient in beta 2M, MHC class I proteins, and CD8+ T cells. Science 1990; 248: 1227–30.

Kontgen F, Suss G, Stewart C, Steinmetz M, Bluethmann H. Targeted disruption of the MHC class II Aa gene in C57BL/6 mice. Int Immunol 1993; 5: 957–64.

Lee BE, Davies HD. Aseptic meningitis. Curr Opin Infect Dis 2007; 20: 272–7.

Lillie RD, Armstrong C. Pathology of lymphocytic choriomeningitis in mice. Arch Pathol 1945; 40: 141–52.

Logan SA, MacMahon E. Viral meningitis. BMJ 2008; 336: 36–40.

Marker O, Nielsen MH, Diemer NH. The permeability of the blood-brain barrier in mice suffering from fatal lymphocytic choriomeningitis virus infection. Acta Neuropathol 1984; 63: 229–39.

McGavern DB. The role of bystander T cells in CNS pathology and pathogen clearance. Crit Rev Immunol 2005; 25: 289–303.

Merkler D, Horvath E, Bruck W, Zinkernagel RM, Del la Torre JC, Pinschewer DD. "Viral deja vu" elicits organ-specific immune disease independent of reactivity to self. J Clin Invest 2006; 116: 1254–63.

Meyer HM Jr, Johnson RT, Crawford IP, Dascomb HE, Rogers NG. Central nervous system syndromes of "vital" etiology. A study of 713 cases. Am J Med 1960; 29: 334–47.

Mims CA. Intracerebral injections and the growth of viruses in the mouse brain. Br J Exp Pathol 1960; 41: 52–9.

Mombaerts P, Mizoguchi E, Ljunggren HG, Iacomini J, Ishikawa H, Wang L, et al. Peripheral lymphoid development and function in TCR mutant mice. Int Immunol 1994; 6: 1061–70.

Oertle T, van der Haar ME, Bandtlow CE, Robeva A, Burfeind P, Buss A, et al. Nogo-A inhibits neurite outgrowth and cell spreading with three discrete regions. J Neurosci 2003; 23: 5393–406.

Oldstone MB. A suspenseful game of 'hide and seek' between virus and host. Nat Immunol 2007; 8: 325–7.

Olert J, Wiedorn KH, Goldmann T, Kuhl H, Mehraein Y, Scherthan H, et al. HOPE fixation: a novel fixing method and paraffin-embedding technique for human soft tissues. Pathol Res Pract 2001; 197: 823–6.

Perarnau B, Saron MF, San Martin BR, Bervas N, Ong H, Soloski MJ, et al. Single H2Kb, H2Db and double H2KbDb knockout mice: peripheral CD8+ T cell repertoire and anti-lymphocytic choriomeningitis virus cytolytic responses. Eur J Immunol 1999; 29: 1243–52.

Peschon JJ, Torrance DS, Stocking KL, Glaccum MB, Otten C, Willis CR, et al. TNF receptor-deficient mice reveal divergent roles for p55

and p75 in several models of inflammation. J Immunol 1998; 160: 943–52.

Pinschewer DD, Perez M, Sanchez AB, de la Torre JC. Recombinant lymphocytic choriomeningitis virus expressing vesicular stomatitis virus glycoprotein. Proc Natl Acad Sci USA 2003; 100: 7895–900.

Pinschewer DD, Perez M, Jeetendra E, Bachi T, Horvath E, Hengartner H, et al. Kinetics of protective antibodies are determined by the viral surface antigen. J Clin Invest 2004; 114: 988–93.

Rubin H, Lehan PH, Doto IL, Chin TD, Heeren RH, Johnson O, et al. Epidemic infection with Coxsackie virus group B, type 5. I. Clinical and epidemiologic aspects. N Engl J Med 1958; 258: 255–63.

Thomsen AR. Lymphocytic choriomeningitis virus-induced central nervous system disease: a model for studying the role of chemokines in regulating the acute antiviral CD8+ T-cell response in an immune-privileged organ. J Virol 2009; 83: 20–8.

Tishon A, Lewicki H, Andaya A, McGavern D, Martin L, Oldstone MB. CD4 T cell control primary measles virus infection of the CNS: regulation is dependent on combined activity with either CD8 T cells or with B cells: CD4, CD8 or B cells alone are ineffective. Virology 2006; 347: 234–45.

Wherry EJ, Ahmed R. Memory CD8 T-cell differentiation during viral infection. J Virol 2004; 78: 5535–45.

Wilsnack RE, Rowe WP. Immunofluorescent studies of the histopathogenesis of lymphocytic choriomeningitis virus infection. J Exp Med 1964; 120: 829–40.

Zinkernagel RM, Doherty PC. Restriction of in vitro T cell-mediated cytotoxicity in lymphocytic choriomeningitis within a syngeneic or semiallogeneic system. Nature 1974; 248: 701–2.